
*17th World Conference on Earthquake Engineering, 17WCEE*
*Sendai, Japan - September 13th to 18th 2020*

# SESIMIC ASSESSMENT OF TALL PIER BRIDGES USING ROKCING FOUNDATION RETROFITTED WITH INERTER SYSTEM

X. Chen[(1)], C. Li[(2)]

[(1)] *Post-doctor, school of mechanism and engineering science/ department of civil engineering, Shanghai University, xuchen_shu@163.com*
[(2)] *Professor, department of civil engineering, Shanghai University, li-chunxiang@vip.sina.com*

***Abstract:*** Due to the mountainous topography, a large amount of bridges contains piers over 40 m have been constructed in **s**outhwest China. This area is known as a region with high seismic hazard level, experiencing several catastrophic earthquakes in recent decade. Current numerical and experimental researches have shown that higher-order modes of columns significantly affected the seismic performance of tall piers; multiple plastic hinges, rather than a single one as specified in current codes, would form along the height when strong earthquakes were considered. Since these tall pier bridges are usually the key links in local highway network, extensive nonlinear performance might have negative influence on post-earthquake rescue operations. Therefore, dynamic control approaches and devices can be employed to mitigate the seismic demands and improve the performance of these bridges. Rocking foundation has been regarded as one of effective isolation approaches alleviating the seismic demands of bridges recently, especially for those with tall piers, **for which** traditional isolation devices (e.g., lead rubber bearing (LRB), viscous dampers) cannot provide satisfying efficiency. However, while pier columns mainly remain elastic during earthquakes when rocking foundations are adopted, excessive rocking angle could be observed, which might lead to overturning of the bridge systems. To overcome the potential instability of rocking foundations, a series-parallel inerter system (SPIS) is utilized in this study to retrofit tall piers with rocking foundation against excessive rocking angle. A typical tall pier bridge system in southwest China is considered and simulated using finite element model. Then the mechanism, simulation and design of this inerter system are introduced sequentially. Finally, both nonlinear time history and fragility analyses are utilized to verify the efficiency of inerter system in mitigating the seismic-induced rocking angle, in terms of deterministic and probabilistic manner, respectively. The time history results show that the rocking angle at pier base could be suppressed when inerter system are design with carefully determined parameters. Furthermore, the effectiveness of this retrofit approach is validated by the probabilistic method with results presented in the format of fragility curves as well. The well-designed inerter system is shown to be capable of reducing the probability of overturning of the rocking foundation.

***Keywords:*** tall pier bridges; seismic control; rocking foundation; inerter system



 




## Introduction

Due to the mountainous topography in southwest China, numerous bridges constructed in recent decades contain tall piers with heights over 40 m. This region is known with high seismic hazard level, which has experienced several catastrophic earthquakes, such as M8.0 Wenchuan earthquake in 2008 and M7.0 Lushan earthquake in 2013. Note that these tall pier bridges are usually key links in local highway network, which function as lifelines in post-earthquake rescue operations by allowing the passage of emergency vehicles. The seismic performance and safety of these bridges are thus of great concern and should be investigated.

Unfortunately, current specifications for seismic design of bridges are generally concentrated on those conventional ones with short-to-mediate piers and invalid for bridges with tall piers as in southwest China. Guan, et al [1] conducted nonlinear time history analysis for a typical bridge with 50 m-height piers, using numerical models with lumped plastic hinges. The results showed that due to the higher-order modes of piers, additional plastic hinge regions might form at the mid-height, which contradicted with the assumption in current codes that plastic deformation would only develop at the base of bridge piers. Through numerical analysis of models with fiber elements, Chen, et al [2] pointed out that the displacement at the top was not highly correlated to the section curvature at the base, indicating that the displacement could not be employed as damage index in the case of tall pier bridges. The authors also found that the shear force and bending moment along the height of tall piers were different from those assumed in design codes. More recently, shake table tests were reported investigating the seismic performance of tall piers in Tongji University [3]; all the aforementioned conclusion from numerical analysis were observed and verified by the recorded experimental results.

All the investigations cited above demonstrated that when subjected to rare earthquakes with great intensities, these tall pier bridges might experience significant nonlinear deformation [4-6]. Since they might be the only access to towns in mountainous areas and were essential for the rescue operations, seismic isolation devices are desired to improving the performance of these bridges against earthquake events. In current engineering practice, laminated rubber bearings (e.g., lead rubber bearings (LRB) and high-damping rubber bearings (HDRB)) are the most widely employed devices mitigating the seismic demands [7]. These bearings could effectively limit the accumulation of seismic inertial force of super-structures, and thus, the damage of pier columns and foundations could be alleviated. These bearings are efficient for conventional bridges with short-to-mediate piers, in which the inertial force of piers is negligible compared with that of



 




girders. However, in the case of tall pier bridges considered herein, the distributed mass of slender columns could be greater than that of super-structures [3]; therefore, the laminated bearings would not perform that well in these siutations.

Rocking foundations might be a promising approach mitigating the seismic demands of tall piers, since this construction strategy could reduce the inertial force of pier columns [8]. Previous investigations [9, 10] showed that rocking foundations could significantly improve the seismic resilience of bridge systems, and the columns might remain elastic even under rare earthquakes. Furthermore, rocking foundations have already been used in some existing bridges with tall piers, e.g., Rio Vista Bridge [11], North Approach Viaduct of Lions Gate Bridge [12] and South Rangitikei Rail Bridge [13]. However, one of the most crucial issues that should be considered in design of this type of foundations is the overturning stability, especially for tall pier bridges.

In recent decades, a new type of energy dissipation device called inerter has been applied to civil structures [14-16]. The inerters possess mass-enhancing mechanism, and thus could function as tuned mass dampers (TMDs) with small actual mass [17]. Unlike traditional TMDs, inerter is a two-end device, and its reaction force is proportional to the relative acceleration between two terminals [18]. The efficiency of inerters in controlling the seismic demands of structures have been demonstrated by various researches [19, 20]. Ikago, et al. [21] and Pan and Zhang [22] investigated the seismic performance of single-of-degree-freedom (SDOF) systems designed with inerter systems. These authors pointed out that the dynamic responses were significantly suppressed by inerters, and they further developed design methods for these systems. Lazar, et al. [23] conducted experiments for inerter systems and the results showed that those inerter elements could generate thousands of times apparent mass than original actual mass, proving to be an efficient vibration mitigation device.

This paper preliminary investigates the effectiveness of a serial-parallel inerter system (SPIS) in improving the overturning stability of rocking foundations in the case of tall pier bridges. The mechanism, simulation and design of the SPIS are introduced sequentially. Both nonlinear time history and fragility analyses are utilized to verify the efficiency of SPIS in mitigating the seismic-induced tilt angle at pier base, in terms of deterministic and probabilistic manner, respectively.



 



## Bridge prototype and numerical models

### Description of the bridge

A typical bridge with tall pier in southwest China is considered in this paper as the prototype, as shown in Figure 1. The superstructure of this prototype bridge consists of 30 m-span continuous concrete girders, while the substructure (pier columns) is composed of variable hollow sections with height around 50 m. The external section dimensions at pier top is 2.1 m × 5.0 m, and the wall thickness is 0.6 m along the height; the inclination of frontal walls is 1/80. More details about this prototype bridge could be referred to in paper [3].

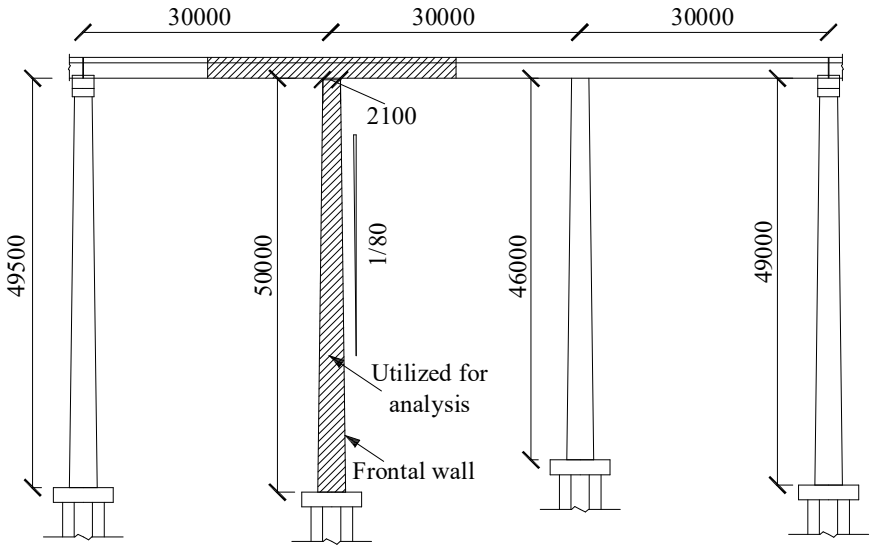


Figure 1 Elevation of the prototype bridge (unit: mm)

Figure 2 shows the rocking foundation for this bridge, while the series-parallel inerter system (SPIS) are plotted for illustration as well. Simulation of the SPIS in the numerical analysis model and determination of the corresponding parameters will be introduced in the following sections.

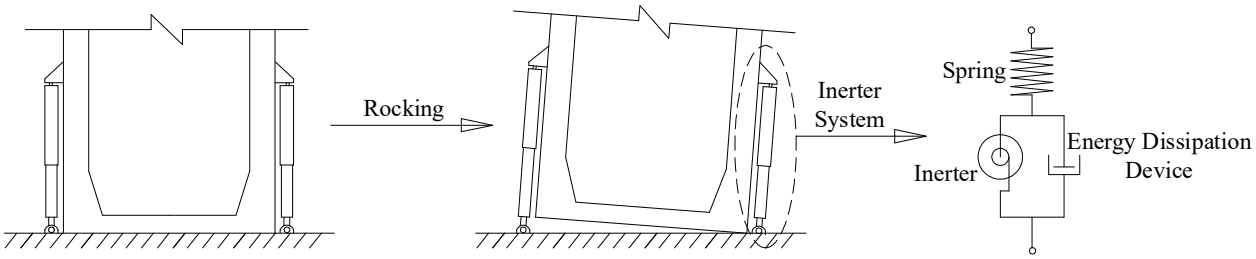


Figure 2 Sketch of rocking foundation retrofitted with series-parallel inerter system (SPIS)



 



**Simulation of the bridge components and SPIS**

The shadowed part of the prototype bridge shown in Figure 1 is utilized for analysis and simplified as a cantilever single-column system, capturing the main characteristics of tall piers with considerable slenderness [5]. As shown in Figure 3 (a), the lumped mass $M_s$ at the top means the tributary masses of super-structures from adjacent two half spans, while the distributed mass of pier columns are designated at element nodes ($m_i$); $\alpha(x)$ and $R(x)$ denote the shape angle and shape parameter [24] of the section located at the height of $x$ measured from rocking base, respectively. When subjected to mild earthquakes, rocking may not initiate and the pier column could remain in contact phase (see in Figure 3 (b)); while strong excitations are considered, uplift could be observed for the rocking foundation, as presented in Figure 3 (c).

To consider the potential nonlinear behavior, fiber elements in *OpenSees* are used simulating pier columns. The cross sections are divided into concrete (core/ cover) fibers and steel fibers (Figure 3 (d)); the constitutive relationships of steel and concrete materials are modelled by Giuffré-Menegotto-Pinto and Kent-Scott-Park models, respectively, as plotted in Figure 3 (e) and (f).

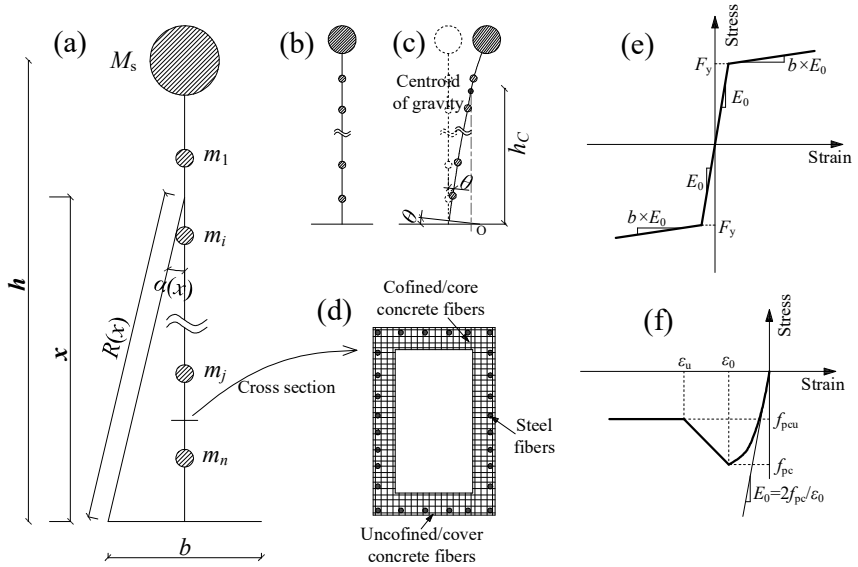


Figure 3 Finite element model: (a) simplified system; (b) contact phase; (c) rocking phase; (d) fiber section; constitutive relationships of (e) steel & (f) concrete materials

Springs without tension strength are employed considering the performance of rocking interface [25], which are simulated by elastic-no-tension (ENT) materials in *OpenSees*. According to FEMA 356 [26], the stiffness of per unit area is computed based on its location, as presented in Figure 4 and Eq. (1 ~ 2).

$$k_{\text{zone 1\&2}} = 6.83G/(1 - \nu) \tag{2}$$



 



$$k_{\text{zone 3}} = 0.73G/(1 - \nu) \quad (3)$$

where G and $\nu$ denote the shear modulus and Poisson's ratio of the material for rocking interface, respectively.

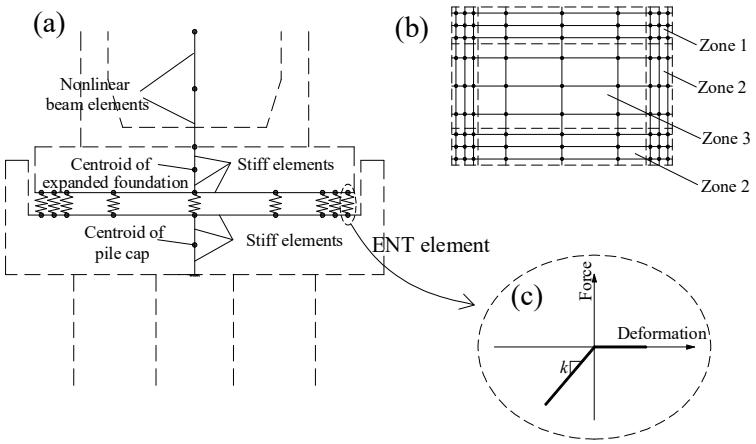


Figure 4 Simulation of rocking foundation: (a) elevation; (b) plan; (c) constitutive relationship of ENT springs

To date, no specific element has been developed simulating the dynamic performance of SPIS. Thus, this system is considered by an equivalent model as presented in Figure 5, which has been proved efficient; more details about this equivalent model could be found in the paper of Ikago, et al [19].

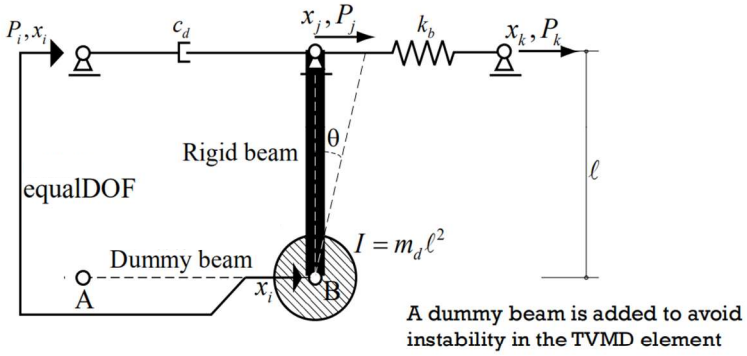


Figure 5 Equivalent system for simulation of SPIS

**Determination of the parameters of SPIS**

The performance of SPIS is dominated by its mass ($m_{\text{in}}$), damping ($c_{\text{in}}$) and stiffness ($k_{\text{in}}$), which are usually expressed by three dimensionless parameters as presented in Table 1 [19]. To find out the optimal values of these design parameters, simple parametric analyses are conducted in this section. Considering the feasibility of construction in engineering practice, several values of $\mu$, $\xi$ and $\kappa$, as presented in Table 1, are employed during analysis. Note that $\kappa$ is described as 'depending on $\mu$' in this table, which will be explained in the following part.



 



Table 1 Parameters considered in parametric analysis

| Parameter | Definition | Values |
|---|---|---|
| $\mu$ | $m_{in}/m$<br>$m$ is the mass of primary structure | 0.5, 1.0,1.5, 2.0 |
| $\xi$ | $c_{in}/(2m\omega)$<br>$\omega$ is the fundamental circular frequency of primary structure | 0.1, 0.2, 0.3 |
| $\kappa$ | $k_{in}/k$<br>$k$ is the stiffness of primary structure | Depending on $\mu$ |

In this preliminary analysis, the well-known EL-Centro ground motion recorded in 1940 Imperial Valley earthquake is utilized as input, exploring the influence of these parameters on the seismic tilt angle at pier base (i.e., $\theta$ in Figure 3 (c)). Figure 6 shows the seismic responses of normalized tilt angle, i.e., $\theta/\alpha_c$, in which $\alpha_c$ is the shape angle corresponding to the centroid of gravity. Note that the parameter of $\omega_{in}/\omega$ is used for lateral axis in this figure, which means the ratio between the circular frequencies of SPIS and primary structure. Since $\omega_{in}$ is defined as $\sqrt{k_{in}/m_{in}}$, the corresponding $\kappa$ could be computed using the value of $\mu$.

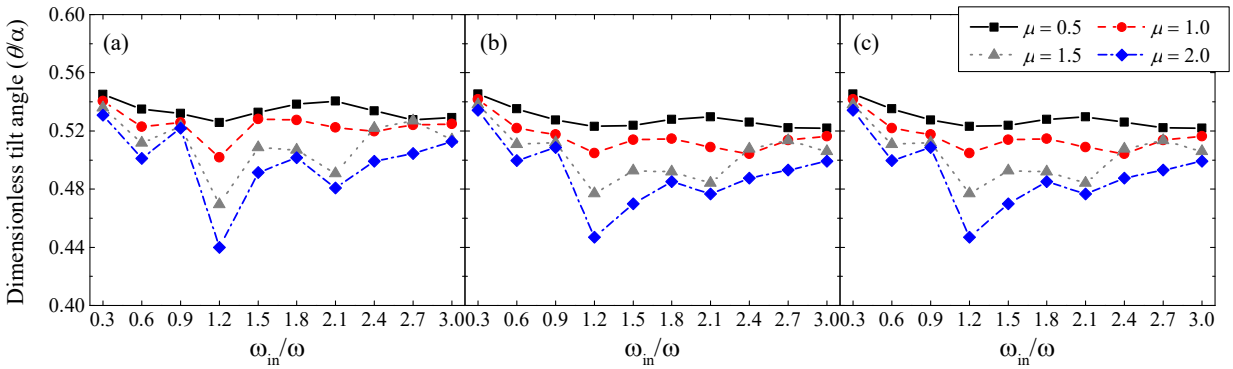


Figure 6 Influence of parameters on normalized tilt angle ($\theta/\alpha_c$): (a) $\xi = 0.1$; (b) $\xi = 0.2$; (c) $\xi = 0.3$

From all scenarios presented in Figure 6, the efficiency of SPIS is observed increase with the value of $\mu$; i.e., a greater $\mu$ generally leads to lower values of $\theta/\alpha_c$. Additionally, the minimum value of $\theta/\alpha_c$ approximately corresponds to the $\omega_{in}/\omega$ of 1.2, regardless the values of $\mu$ and $\xi$. On the other hand, comparing the results corresponding to different $\xi$ values, the efficiency of SPIS mainly remains similar. For example, with $\mu$ of 2.0, the minimum values of $\theta/\alpha_c$ are 0.440 and 0.450, respectively, for $\xi$ equaling 0.1 and 0.3. Consequently, the values of $\mu$, $\xi$ and $\kappa$ are determined as 2.0, 0.1 and 2.88 (corresponding to $\omega_{in}/\omega$ for of 1.2), respectively, in the following analysis procedures, considering both the convenience of construction and economic cost.



 



## Selection of ground motions

A suite of 7 typical ground motions are selected from Pacific Earthquake Engineering Center (PEER) database and utilized as input in this study; detailed information of these motions is presented in Table 2. From this table, these motions are observed with PGA levels ranging from 0.006 g to 0.098 g, and epicentral distance over 50 km.

Table 2 Selected input ground motions

| No. | Earthquake | Year | Magnitude | Epicentral Distance ($R_{jb}$, km) | PGA (g) |
|---|---|---|---|---|---|
| E1 | San Fernando | 1971 | 6.61 | 61.75 | 0.052 |
| E2 | Taiwan SMART1 | 1983 | 6.50 | 91.54 | 0.006 |
| E3 | Taiwan SMART3 | 1986 | 7.30 | 51.35 | 0.052 |
| E4 | Loma Prieta | 1989 | 6.93 | 79.16 | 0.049 |
| E5 | Loma Prieta | 1989 | 6.93 | 71.23 | 0.098 |
| E6 | Landers | 1992 | 7.28 | 144.13 | 0.026 |
| E7 | Landers | 1992 | 7.28 | 50.85 | 0.050 |

During the deterministic time history analyses, the input PGA level of all these selected motions are scaled to 1.5 g, simulating the rare earthquake excitations observed and recorded in Wenchuan earthquake in southwest China. While for the fragility analysis, 10 scaling factors uniformly distributed from 0.2 to 2.0 are employed for the original motions listed in Table 2, providing sufficient data for developing more reliable probabilistic seismic demand models (PSDMs).

## Analysis results

The analysis results are presented and discussed in this section. A widely used fragility analysis procedure is utilized in this paper, which will not be introduced in detail herein; more information about this procedure could be referred to in various papers [5, 27, 28].

Figure 7 plots and compares the $\theta/\alpha_c$ values of rocking foundations with and without SPIS for each of the input motions; the reduction ratio for each case is presented for illustration as well. This figure shows that the seismic demands are reduced when inerter systems are implemented, and the reduction ratios are generally around -10% with an average value of -12.3%. Note that the SPIS is not that effective as in the case for EL-Centro motion, where the reduction ratio could reach 20%, as shown in Figure 7. The reason might be that the values of design parameters (i.e., $\mu$, $\xi$ and $\kappa$) for SPIS are related to the characteristics



 



(e.g., frequency contents) of input motions, and a more comprehensive procedure should be conducted to obtain the optimal values of $\mu$, $\xi$ and $\kappa$.

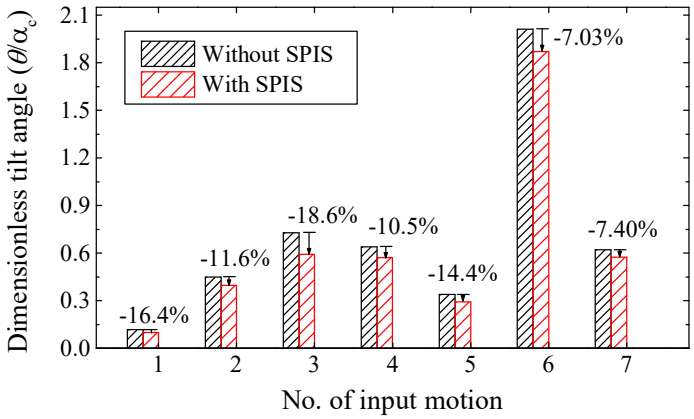


Figure 7 $\theta/\alpha_c$ of piers with and without SPIS for each motion (PGA = 1.5 g)

According to previous study, the value of $\theta/\alpha_c$ corresponding to overturning was estimated as 1.08. Thus, this value is utilized as the threshold of overturning damage state when developing the fragility curve. Figure 8 (a) and (b) present and compare the probabilistic seismic demand models (PSDMs) and fragility curves for tall piers with and without SPIS, respectively. The results of regression analysis developing PSDMs are shown in Figure 8 (a) as well for illustration. In these figures, the input PGA is employed as intensity measure (IM) and the normalized tilt angle, $\theta/\alpha_c$, is utilized as damage measure, respectively.

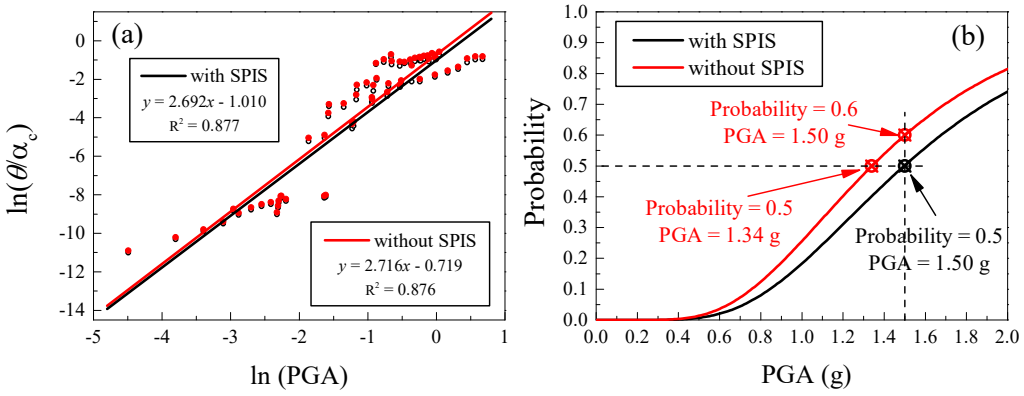


Figure 8 PSDMs and fragility curves

Figure 8 (a) shows that the $R^2$ of PSDMs for both tall pier systems are over 0.85, indicating that the linear regression analysis is appropriate for the scenarios considered in current investigation. From this figure, the PSDM of the pier with SPIS is observed yielding lower demands than that of the original system



 




for the whole PGA range considered. This fact indicates that the mean seismic responses of $\theta/\alpha_c$ are expected to be suppressed by the implementation of SPIS. While Figure 8 (b) shows that the probability of overturning is reduced by the employment of SPIS as well. For example, the PGA corresponding to 50% probability of being damaged (overturning herein) is 1.34 g for the original tall pier column, while that value for the system implemented with SPIS is 1.50 g. On the other hand, when input PGA equals 1.50 g, as employed for deterministic analysis, the probabilities of overturning for the rocking foundation with and without SPIS are 0.50 and 0.60, respectively. These phenomena are consistent with those obtained from previous deterministic time history analysis, again verifying the effectiveness of SPIS in improving the overturning stability of rocking foundations adopted for tall piers.

## Conclusions

This paper investigates the effectiveness of a serial-parallel inerter system (SPIS) controlling the tilt angle of rocking foundations adopted in tall piers. Both deterministic and probabilistic analyses are conducted, and the corresponding seismic responses are obtained and compared.

From the results, the efficiency of SPIS is observed significantly influenced by its apparent mass and stiffness, which are represented by $\mu$ and $\kappa$ in this paper; while the effects of damping ($\xi$) are less important compared with $\mu$ and $\kappa$. Therefore, the design values of $\mu$, $\xi$ and $\kappa$ are determined as 2.0, 0.1 and 2.88, respectively, considering both the efficiency of vibration mitigation and feasibility of construction. Furthermore, examination of the normalized tilt angle demands ($\theta/\alpha_c$) shows that the seismic responses and probability of overturning of rocking foundations could be effectively reduced through utilization of SPIS. Therefore, this inerter system is proved a promising approach improving the seismic performance of tall pier bridges using rocking foundations.

Note that the design parameters of the SPIS employed in current paper were determined from a preliminary parametric analysis, in which only the EL-Centro input motion is incorporated. More detailed investigations about the optimal parameters of SPIS will be conducted, accounting for more generalized scenarios. Furthermore, only the overturning of rocking foundations is considered herein, due to the lack of researches focusing on various quantified damage states of this type of foundations. More work should be conducted for these issues in the future.



 




## Acknowledgement

The authors gratefully acknowledge the support by the China Postdoctoral Science Foundation (No. 2019M651468) and the National Natural Science Foundation (No. 51908348). The first author also acknowledges the support of *Shanghai Post-doctoral Excellence Program*.

## References

[1] Guan Z, Li J, Xu Y, Lu H. Higher-order mode effects on the seismic performance of tall piers. Frontiers of Architecture Civil Engineering in China. 2011;5:496-502.

[2] Chen X, Li J, Guan Z. Effects of higher modes on tall piers. IABSE Symposium Report: International Association for Bridge and Structural Engineering; 2016. p. 136-43.

[3] Chen X, Guan Z, Li J, Spencer Jr BF. Shake table tests of tall-pier bridges to evaluate seismic performance. Journal of Bridge Engineering. 2018;23:04018058.

[4] Chen X, Guan Z, Spencer Jr BF, Li J. A simplified procedure for estimating nonlinear seismic demand of tall piers. Engineering Structures. 2018;174:778-91.

[5] Chen X, Li J, Guan Z. Fragility analysis of tall pier bridges subjected to near-fault pulse-like ground motions. Structure and Infrastructure Engineering. 2019:1-14.

[6] Chen X. System Fragility Assessment of Tall-Pier Bridges Subjected to Near-Fault Ground Motions. Journal of Bridge Engineering. 2020;25:04019143.

[7] Abe M, Yoshida J, Fujino Y. Multiaxial behaviors of laminated rubber bearings and their modeling. I: experimental study. Journal of Structural Engineering. 2004;130:1119-32.

[8] Nguyen W, Trono W, Panagiotou M, Ostertag CP. Seismic response of a rocking bridge column using a precast hybrid fiber-reinforced concrete (HyFRC) tube. Composite Structures. 2017;174:252-62.

[9] Hung HH, Liu KY, Ho TH, Chang KC. An experimental study on the rocking response of bridge piers with spread footing foundations. Earthquake Engineering and Structural Dynamics. 2011;40:749-69.

[10] Xie Y, Zhang J, DesRoches R, Padgett JE. Seismic fragilities of single-column highway bridges with rocking column-footing. Earthquake Engineering and Structural Dynamics. 2019;48:843-64.

[11] Yashinsky M, Karshenas M. Fundamentals of seismic protection for bridges: National Information Centre of Earthquake Engineering, 2003.

[12] Dowdell DJ, Hamersley BA. Lions' gate bridge north approach: seismic retrofit. Behaviour of Steel Structures in Seismic Areas: Proc, 3rd Int Conf: STESSA 2000: Balkema; 2000. p. 319-26.

[13] Beck J, Skinner R. The seismic response of a reinforced concrete bridge pier designed to step. Earthquake Engineering and Structural Dynamics. 1973;2:343-58.

[14] De Domenico D, Ricciardi G. Improving the dynamic performance of base-isolated structures via tuned mass damper and inerter devices: A comparative study. Structural Control & Health Monitoring. 2018;25:e2234.



 




[15] Giaralis A, Taflanidis A. Optimal tuned mass-damper-inerter (TMDI) design for seismically excited MDOF structures with model uncertainties based on reliability criteria. Structural Control & Health Monitoring. 2018;25:e2082.

[16] De Domenico D, Ricciardi G. Optimal design and seismic performance of tuned mass damper inerter (TMDI) for structures with nonlinear base isolation systems. Earthquake Engineering and Structural Dynamics. 2018;47:2539-60.

[17] Arakaki T, Kuroda H, Arima F, Inoue Y, Baba K. Development of seismic devices applied to ball screw. Part 1: Basic performance test of RD-series. AIJ Journal of Technology Design. 1999;5:239-44.

[18] Zhang R, Zhao Z, Dai K. Seismic response mitigation of a wind turbine tower using a tuned parallel inerter mass system. Engineering Structures. 2019;180:29-39.

[19] Ikago K, Saito K, Inoue N. Seismic control of single-degree-of-freedom structure using tuned viscous mass damper. Earthquake Engineering and Structural Dynamics. 2012;41:453-74.

[20] Pan C, Zhang R, Luo H, Li C, Shen H. Demand-based optimal design of oscillator with parallel-layout viscous inerter damper. Structural Control & Health Monitoring. 2018;25:e2051.

[21] Ikago K, Sugimura Y, Saito K, Inoue N. Simple design method for a tuned viscous mass damper seismic control system. Proceedings of the 15th World Conference on Earthquake Engineering, Lisbon, Portugal, Paper ID2012.

[22] Pan C, Zhang R. Design of structure with inerter system based on stochastic response mitigation ratio. Structural Control & Health Monitoring. 2018;25:e2169.

[23] Lazar I, Neild S, Wagg D. Using an inerter-based device for structural vibration suppression. Earthquake Engineering and Structural Dynamics. 2014;43:1129-47.

[24] Thiers-Moggia R, Málaga-Chuquitaype C. Seismic protection of rocking structures with inerters. Earthquake Engineering and Structural Dynamics. 2019;48:528-47.

[25] Antonellis G, Panagiotou M. Seismic response of bridges with rocking foundations compared to fixed-base bridges at a near-fault site. Journal of Bridge Engineering. 2014;19:04014007.

[26] FEMA 356. Prestandard and commentary for the seismic rehabilitation of buildings. American Society of Civil Engineers. 2000.

[27] Padgett JE, DesRoches R. Methodology for the development of analytical fragility curves for retrofitted bridges. Earthquake Engineering and Structural Dynamics. 2008;37:1157-74.

[28] Alam MS, Bhuiyan MR, Billah AM. Seismic fragility assessment of SMA-bar restrained multi-span continuous highway bridge isolated by different laminated rubber bearings in medium to strong seismic risk zones. Bulletin of Earthquake Engineering. 2012;10:1885-909.

[29] Thiers‐Moggia R, Málaga‐Chuquitaype C. Seismic protection of rocking structures with inerters. Earthquake engineering and structural dynamics. 2019.



 